IEEE Photonics Journal
An IEEE Photonics Society Publication

Open Access

All-Optical Generation of Two IEEE802.11n Signals for 2 × 2 MIMO-RoF via MRR System

Volume 6, Number 6, December 2014

I. S. Amiri
S. E. Alavi
N. Fisal
A. S. M. Supa'at
H. Ahmad

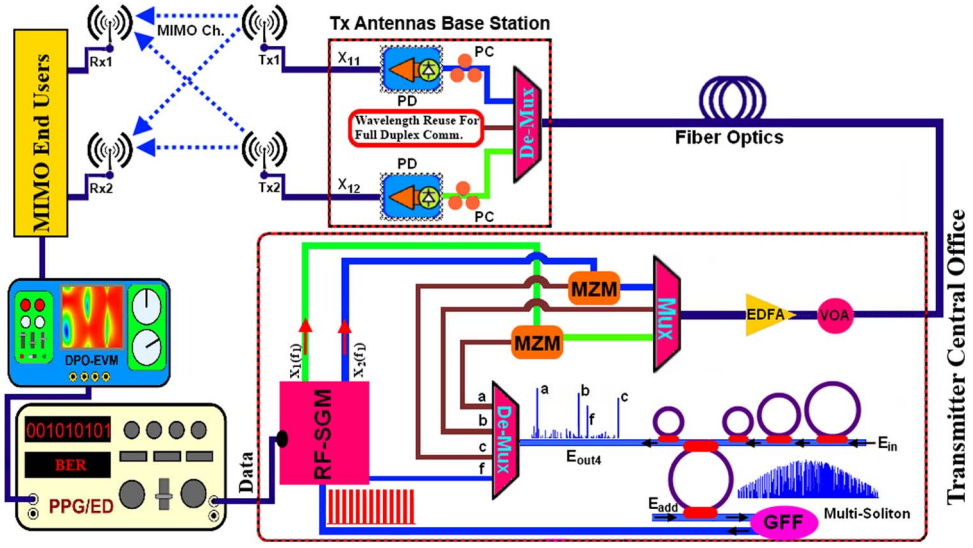

DOI: 10.1109/JPHOT.2014.2363437
1943-0655 © 2014 IEEE

All-Optical Generation of Two IEEE802.11n Signals for 2 × 2 MIMO-RoF via MRR System

I. S. Amiri,[1] S. E. Alavi,[2] N. Fisal,[2] A. S. M. Supa'at,[3] and H. Ahmad[1]

[1]Photonics Research Centre, University of Malaya, 50603 Kuala Lumpur, Malaysia
[2]UTM MIMOS CoE in Telecommunication Technology Faculty of Electrical Engineering, Universiti Teknologi Malaysia (UTM), 81310 Johor Bahru, Malaysia
[3]Lightwave Communication Research Group, Faculty of Electrical Engineering, Universiti Teknologi Malaysia (UTM), 81310 Johor Bahru, Malaysia

DOI: 10.1109/JPHOT.2014.2363437

Manuscript received September 10, 2014; accepted October 11, 2014. Date of publication October 14, 2014; date of current version October 27, 2014. This work was supported by the Ministry of Higher Education (MOHE), Malaysia, and Research Management Center (RMC), Universiti Teknologi Malaysia (UTM), under Research Grant R.J130000.7823.4L145. The work of I. S. Amiri and H. Ahmad was supported by the University of Malaya/MOHE under Grant UM.C/625/1/HIR/MOHE/SCI/29 and Grant RU002/2013. Corresponding author: S. E. Alavi (e-mail: sayedehsan@utm.my).

Abstract: A radio-over-fiber system capable of very spectrally efficient data transmission and based on multiple-input multiple-output (MIMO) and orthogonal frequency-division multiplexing (OFDM) is presented here. Carrier generation is the basic building block for implementation of OFDM transmission, and multicarriers can be generated using the microring resonator (MRR) system. A series of MRRs incorporated with an add/drop filter system was utilized to generate multicarriers in the 193.00999–193.01001-THz range, which were used to all-optically generate two MIMO wireless local area network radio frequency (RF) signals suitable for the IEEE802.11n standard communication systems, and single wavelengths at frequencies of 193.08, 193.1, and 193.12 THz with free spectral range of 20 GHz used to optically transport the separated MIMO signals over a single-mode fiber (SMF). The error vector magnitude (EVM) and bit error rate of the overall system performance are discussed. Results show that the generated RF signals wirelessly propagated through the MIMO channel using the 2 × 2 MIMO Tx antennas. There is an acceptable EVM variation for wireless distance lower than 70, 30, and 15 m. It can be concluded that the transmission of both MIMO RF signals is feasible for up to a 50-km SMF path length and a wireless distance of 15 m.

Index Terms: IEEE802.11n, MIMO, OFDM, Radio over Fiber (RoF).

1. Introduction

Wireless communication with higher data rates is becoming greatly important to end users [1]. In this regard, radio-over-fiber (RoF) technology is deployed in wireless networks in order to provide an increase in capacity and quality of service, and possesses a combination of the flexibility and mobility of wireless access networks with the capacity of optical networks [2]. Another approach to increase data rates lies in the development of spatial diversity antenna systems in a multiple-input and multiple-output (MIMO) configuration [3], which is widely used in wireless communication systems [4]. A combination of RoF and MIMO thus has the potential to significantly enhance system efficiency. Wireless signal transportation in the RoF-MIMO system has

several drawbacks, including dispersion effects in the fiber link and multipath fading in the wireless link [5], [6]. The spectrally efficient orthogonal frequency-division multiplexing (OFDM) transmission is a means to eliminate intersymbol interference (ISI) caused by dispersive channels [7]. OFDM has the advantage of robustness against wireless frequency-selective fading channels, and possesses inherent high chromatic dispersion tolerance in optical fibers. Exploiting the diversity in both the frequency and the space domains of an OFDM-MIMO combination could result in exceptional system performance [8]. Furthermore, integrating MIMO-OFDM with RoF provides the possibility of very spectrally efficient data transmission, thereby meeting the high-speed requirements of future generations of wireless systems [9]. MIMO-OFDM-RoF communication systems employ multiple antenna arrays distributed around a micro/femto cell and connected to a central base station via optical fiber [10]. In MIMO, several radio channels are transported between the central unit and the remote units with exactly the same radio carrier frequency [11]. Distinct RoF signals with the same frequency yet separate optical wavelengths can be transported on the same fiber. In this work, these separated wavelengths are generated using the microring resonators (MRRs) instead of requiring several optical sources.

An OFDM system includes an inverse fast Fourier transform (IFFT) block at the transmitter and a fast Fourier transform (FFT) block at the receiver. These blocks are usually implemented in the electrical domain via high-speed digital-signal-processing (DSP) devices, though such enabling devices are commercially and technically challenging. Investigations to reduce the challenges presented by implementation into the electrical domain have resulted in increasing attention being paid to all-optical techniques, which are based on the optical generation and processing of OFDM signals by means of passive optical devices [12], [13]. Transmission of all-optical OFDM is implemented by first generating multiple optical subcarriers, separating these subcarriers via optical devices, and finally modulating each subcarrier separately [14], [15]. Optical carrier generation thus constitutes the basic building block to implement OFDM transmission fully in the optical domain. The MRR system provides a viable means to generate this building block that represents the generation of the necessary multi-carriers. The application of the MRR system in the work described here is two-fold. Firstly, MRR is utilized to generate multi wavelength carriers for transporting several MIMO-RoF signals over a fiber link, and secondly, the generated multi-carriers are used to construct an OFDM signal suitable for the IEEE802.11n standard communication systems. Non-linear light behavior inside an MRR occurs when a strong pulse of light is inputted into the ring system [16]. The properties of a ring system can be modified via various control methods, and ring resonators possessing suitable system parameters can be used as filter devices during generation of high-frequency (THz) soliton signals [17]. The technique of MRRs connected in series and incorporated with an add/drop filter system is utilized in many applications in optical communication and signal processing. A soliton solution of the nonlinear wave equation is always stable over a long distance link, and this stability of soliton signals is even more remarkable than the possibility of balancing dispersion and nonlinearity. As such, a soliton shape can adiabatically adapt in response to slowly varying parameters of the medium [18].

One important aspect of the MRR system is that suitable tuning of the system parameters allows for desired soliton carriers with specific key characteristics, such as full width at half maximum (FWHM) and stability, to be obtained at the drop/through ports of the system. These soliton pulses have sufficiently stability for preservation of their shape and velocity while travelling along the medium [19]–[21]. The advantage of the proposed system is that the transmitter can be fabricated on-chip or operated by a single device. Market acceptance of laser sources is currently limited owing to shortcomings such as restricted tunability range and cumbersome size, although emerging new classes of tunable fiber laser setups are eradicating such constraints. Technological progress in fields such as tunable narrow band laser systems, multiple transmission, and MRR systems constitute a base for the development of new transmission techniques. This paper is organized as follows: Section 2 covers the theoretical background of single and multi-carrier optical soliton pulse generation that is usable in an MIMO-OFDM-RoF system. Results of soliton generation are given in Section 3. Section 4 describes the MIMO-OFDM-RoF system design,

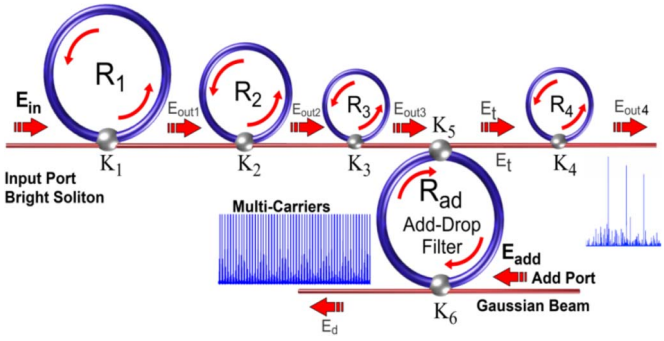

Fig. 1. MRR system overview, with abbreviations R: ring radii, κ: coupling coefficients, R_{ad}: add/drop ring radius, E_{in}, E_{add}: input powers, E_{out}: Ring resonator output E_t: throughput output, and E_d: drop port output.

with the overall view and concepts of the MIMO signal generation and its transmission over SMF optical link and 2 $\times$ 2 MIMO wireless link presented. Section 4.3 contains details of the EVM and BER calculation of overall system performance. In Section 5, the MIMO system is compared with single input single output (SISO) counterpart, and finally, concluding remarks of this work are provided in Section 6.

2. Theoretical Background

Fig. 1 shows the MRR system for THz frequency band generation. Here, a series of MRRs are incorporated into an add/drop filter system. The filtering process of the input soliton pulses is performed via the MRRs, in which pulses of 193–193.2 THz frequency ranges can be obtained. A large output gain is achieved via the soliton self-phase modulation that is required to balance the dispersion effects of the linear medium.

The medium has Kerr effect-type non-linearity. The Kerr effect causes the refractive index (n) of the medium to adhere to the relation [23]

$$n = n_0 + n_2 I = n_0 + \frac{n_2}{A_{eff}} P \tag{1}$$

where n_0 and n_2 are the linear and nonlinear refractive indices respectively, I is the optical intensity, and P represents the optical power. The effective mode core area A_{eff} ranges from 0.10 to 0.50 μm^2 for InGaAsP/InP. A bright soliton and Gaussian beam with a central frequency of 193.1 THz and power of 1.2 W are introduced into the input E_{in} and add E_{add} ports of the system. These optical fields of the optical bright soliton and Gaussian beam are given by [24]

$$E_{in} = A\mathrm{sech}\left[\frac{T}{T_0}\right]\exp\left[\left(\frac{z}{2L_D}\right) - i\omega_0 t\right] \tag{2}$$

$$E_{add}(t,z) == E_0\exp\left[\left(\frac{z}{2L_D}\right) - i\omega_0 t\right] \tag{3}$$

where A and E_0 are the amplitudes of the optical field for the input and add ports respectively, z is the propagation distance, LD is the dispersion length of the soliton pulse, ω_0 is the carrier frequency of the signal and T represents a soliton pulse propagation time. The soliton pulse propagates with a temporal width invariance, and hence it is described as a temporal soliton. A balance should be achieved between L_D and the non-linear length $L_{NL} = 1/\Gamma\phi_{NL}$, where $\Gamma = n_2 \times k$ is the length scale over which disperse or nonlinear effects make the beam become wider or narrower, such that ideally $L_D = L_{NL}$. ϕ_{NL} is the non-linear phase shifts. The normalized

output of the light field, which is the ratio between the output and the input fields for each ring resonator, can be expressed by

$$\left|\frac{E_{out}(t)}{E_{in}(t)}\right|^2 = (1-\gamma) \times \left[1 - \frac{\left(1-(1-\gamma)x^2\right)\kappa}{(1-x\sqrt{1-\gamma}\sqrt{1-\kappa})^2 + 4x\sqrt{1-\gamma}\sqrt{1-\kappa}\sin^2\left(\frac{\phi}{2}\right)}\right] \tag{4}$$

κ is the coupling coefficient, and x represents the round trip loss coefficient, whereby $x = \exp(-\alpha L/2)$ with the ring resonator length L and linear absorption coefficient α. $\phi = \phi_0 + \phi_{NL}$, where $\phi_0 = kLn_0$ and $\phi_{NL} = kLn_2|E_{in}|^2$ are the linear and non-linear phase shifts, respectively [25], [26]. The wave propagation number in a vacuum is $k = 2\pi/\lambda$ while the fractional coupler intensity loss is given by γ. Once the bright soliton pulse is input into the MRRs, a chaotic signal can be formed by application of appropriate parameters. For the add/drop system, the interior electric fields E_a and E_b are expressed as

$$E_a = \frac{E_{out3} \times j\sqrt{\kappa_5}}{1-\sqrt{1-\kappa_5}\sqrt{1-\kappa_6}e^{\frac{-\alpha}{2}L_{ad}-jk_nL_{ad}}} \tag{5}$$

$$E_b = \frac{E_{out3} \times j\sqrt{\kappa_5}}{1-\sqrt{1-\kappa_5}\sqrt{1-\kappa_6}e^{\frac{-\alpha}{2}L_{ad}-jk_nL_{ad}}} \cdot \sqrt{1-\kappa_6}e^{\frac{-\alpha}{2}\frac{L_{ad}}{2}-jk_n\frac{L_{ad}}{2}} \tag{6}$$

where κ_5 and κ_6 are the coupling coefficients, $L_{ad} = 2\pi R_{ad}$, and R_{ad} is the radius of the add/drop system. The throughput and drop port electrical fields of the add/drop system can be expressed by

$$\begin{aligned}\frac{E_t}{E_{out3}} &= \frac{-\kappa_5\sqrt{1-\kappa_6}e^{\frac{-\alpha}{2}L_{ad}-jk_nL_{ad}} + \sqrt{1-\kappa_5} - (1-\kappa_5)\sqrt{1-\kappa_6}e^{\frac{-\alpha}{2}L_{ad}-jk_nL_{ad}}}{1-\sqrt{1-\kappa_5}\sqrt{1-\kappa_6}e^{\frac{-\alpha}{2}L_{ad}-jk_nL_{ad}}} \\ &= \frac{-\sqrt{1-\kappa_6}e^{\frac{-\alpha}{2}L_{ad}-jk_nL_{ad}} + \sqrt{1-\kappa_5}}{1-\sqrt{1-\kappa_5}\sqrt{1-\kappa_6}e^{\frac{-\alpha}{2}L_{ad}-jk_nL_{ad}}}\end{aligned} \tag{7}$$

$$\frac{E_d}{E_{out3}} = \frac{-\sqrt{\kappa_5.\kappa_6}e^{\frac{-\alpha}{2}\frac{L_{ad}}{2}-jk_n\frac{L_{ad}}{2}}}{1-\sqrt{1-\kappa_5}\sqrt{1-\kappa_6}e^{\frac{-\alpha}{2}L_{ad}-jk_nL_{ad}}} \tag{8}$$

and hence the normalized optical outputs of the add/drop system can be expressed by

$$\frac{|E_t|^2}{|E_{out3}|^2} = \frac{(1-\kappa_5) - 2\sqrt{1-\kappa_5}\cdot\sqrt{1-\kappa_6}e^{-\frac{\alpha}{2}L_{ad}}\cos(k_nL_{ad}) + (1-\kappa_6)e^{-\alpha L_{ad}}}{1+(1-\kappa_5)(1-\kappa_6)e^{-\alpha L_{ad}} - 2\sqrt{1-\kappa_5}\cdot\sqrt{1-\kappa_6}e^{-\frac{\alpha}{2}L_{ad}}\cos(k_nL_{ad})} \tag{9}$$

$$\frac{|E_d|^2}{|E_{out3}|^2} = \frac{\kappa_5\kappa_6e^{-\frac{\alpha}{2}L_{ad}}}{1+(1-\kappa_5)(1-\kappa_6)e^{-\alpha L_{ad}} - 2\sqrt{1-\kappa_5}\cdot\sqrt{1-\kappa_6}e^{-\frac{\alpha}{2}L_{ad}}\cos(k_nL_{ad})} \tag{10}$$

where $|E_t|^2$ and $|E_d|^2$ are the output intensities of the through and drop ports respectively, and the output electric field from the third ring is given by E_{out3}. The non-linear refractive index can be neglected for the add/drop system. The throughput output from the add/drop system enters the fourth ring resonator, whereupon the filtering of the signals leads to the generation of ultra-short THz solitons.

3. Results of Soliton Generation

A soliton fiber laser system based on single mode fiber (SMF) was used in this study. The bright soliton was inserted into the system and subsequently round-tripped within the ring resonators.

TABLE 1

Fixed parameters of the MRR system

Fixed	R_{ad}	R_1	R_2	R_3	R_4	κ_1	κ_2	κ_3	κ_4
	100μm	15μm	9μm	6 μm	6 μm	0.98	0.98	0.96	0.92
	κ_5	κ_5	n_0	n_2 (m^2W^{-1})	A_{eff1} (μm^2)	A_{eff2} (μm^2)	A_{eff3-4} (μm^2)	α ($dBmm^{-1}$)	γ
	0.1	0.1	3.34	2.4×10-17	0.50	0.25	0.10	0.5	0.1

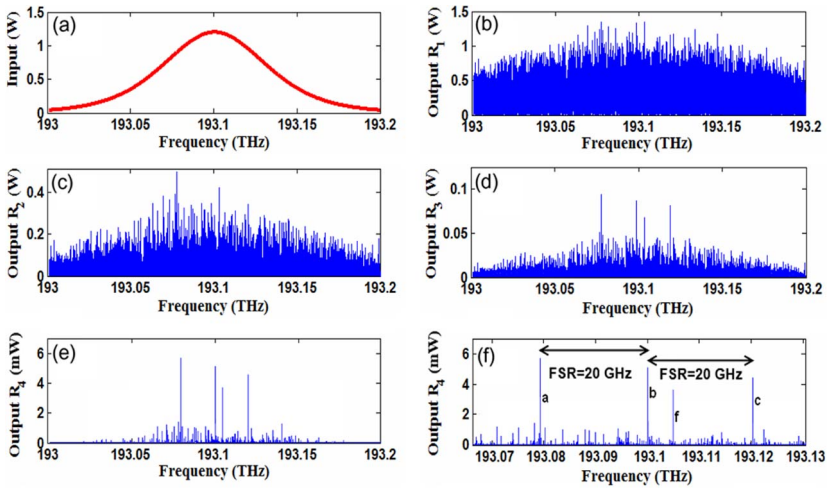

Fig. 2. Results of single and multi-carriers. (a) Input bright soliton. (b) Output from first ring. (c) Output from second ring. (d) Output from third ring. (e) Output from the fourth ring. (f) Expansion of the output R_4.

Each round-trip of the input soliton pulse had a consequent single line frequency as output, and thus the spectrum of the input pulse was split into many single lines frequencies or resulted in the generation of chaotic signals following accumulated round-trips. This mechanism acted as a filtering system in which the intensity accumulated during the round-trips of the input pulse. The fixed parameters of the MRR system are listed in Table 1. The results of the chaotic signal generation are shown in Fig. 2. The input pulse of the bright soliton and Gaussian beam pulse with power of 1.2 W were inserted into the system. Large bandwidth within the MRRs was generated via a bright soliton pulse input into the non-linear system. The signal was chopped (sliced) into smaller signals spreading over the spectrum, and consequently a large bandwidth was formed due to the non-linear effects of the medium. A frequency band of soliton pulses could be formed and trapped within the system when suitable ring parameters are selected. Filtering of the soliton signals was performed when the pulses passed through the MRRs. The output signals from the MRRs, as seen in Fig. 2(b)–(f), were generated with a frequency range of 193–193.2 THz. The fourth MRR's output $(E_{out4}(t))$ shows localized ultra-short soliton pulses at frequencies of 193.08, 193.1, 193.1054, and 193.12 THz in Fig. 2(f). The drop port output, E_d, is shown in Fig. 3. The input Gaussian beam with short bandwidth of 600 MHz into the add port of the system resulted in the generation of multi-soliton pulses ranging from 193.099625 to 193.100375 THz as shown in Fig. 3(a). The range 193.00999–193.01001 THz was selected in this study and used to generate 64 multi-carriers with specific free spectral range (FSR) of 312.5 kHz that was suitable for IEEE802.11n signal generation. These 64 multi-carriers were generated by using a gain flattening filter (GFF) on the multi-solitons with a threshold power of 0.2 mW and are shown in Fig. 3(c) and (d).

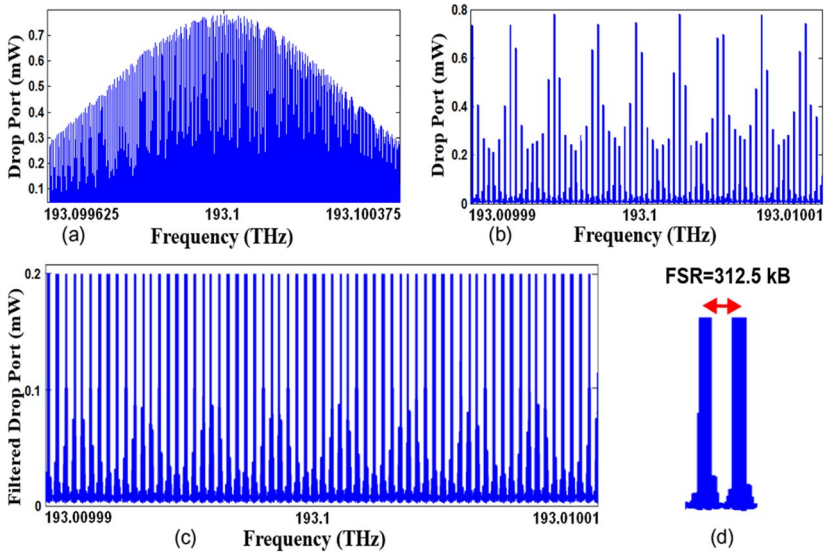

Fig. 3. (a) Multi-solitons output from the drop port. (b) Multi-solitons with range 193.00999–193.01001 THz. (c) 64 multi-carriers generation. (d) FSR of the multi-carriers has the value of 312.5 kHz.

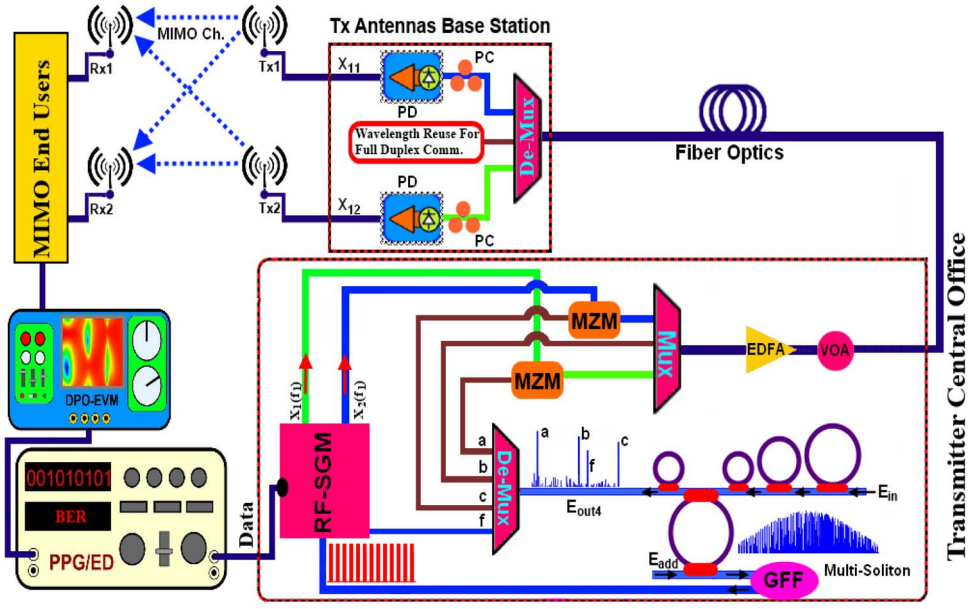

Fig. 4. System setup.

The advantage of using the add/drop filter system is to generate spatially uniform multi-solitons that can be filtered and subsequently utilized as multi-carriers possessing uniformity in both space and power.

4. System Setup

The schematic of the MIMO-OFDM-RoF system setup is shown in Fig. 4. At the transmitter central office (TCO) a series of MRRs were connected to an add/drop system in order to

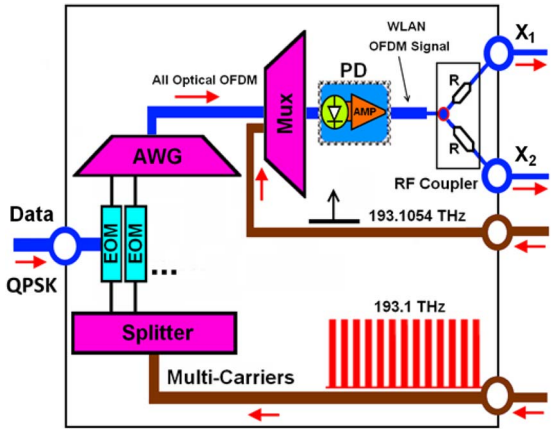

Fig. 5. RF-SGM schematic diagram.

generate single and multi-soliton carriers. As shown in Fig. 2(f), the fourth MRR output generated four carriers which were centered at (a) 193.08, (b) 193.1, (c) 193.12, and (f) 193.1054 THz. These four carriers were separated with a demultiplexer, after which the carrier f was inserted in the RF signal generator module (RF-SGM). The two carriers a and c were assigned for modulating two MIMO signals generated via RF-SGM using Mach-Zehnder optical modulators (MZM), while carrier b was designated for uplink communication.

4.1. MIMO WLAN Signal Generation

The MIMO WLAN signals were generated using the RF-SGM, with the principal operation of the RF-SGM illustrated in Fig. 5. This module had two optical inputs, one electrical input, and two RF output ports. The electrical input port was connected to the pulse pattern generator (PPG) which generated quadrature phase-shift keying (QPSK) data signals. Optical inputs consisted of the single carrier f with frequency 193.1054 THz and the multi-carriers centered at 193.1 THz. In order to generate all optical WLAN MIMO signals, multi-carriers were first separated by the optical splitter and subsequently 52 out of the 64 multi-carriers were modulated via a QPSK signal from the PGG via an external optical modulator (EOM). An array waveguide grating (AWG) was used to characterize the IFFT block at the transmitter and the FFT block at the receiver [15]. We want the optical OFDM signal to have 64 subcarriers with frequency spacing of 312.5 KHz, so the AWG should be a cyclic AWG with 64 channels in the arrayed waveguides, with channel spacing of 312.5 KHz. The FSR of the AWG should be 64×312.5 KHz $= 20$ MHz, implying $\tau = 1/20$ MHz $= 0.5$ ps. Spectra of the modulated optical subcarriers were overlapped, and this resulted in one optical OFDM channel band. Then the generated all-optical OFDM signal was multiplexed by the wavelength of carrier f possessing frequency 193.1054 THz. The distance between a single subcarrier and the center of the multi-carriers was 5.4 GHz, the RF band for the IEEE802.11n standard. After beating the two wavelengths to the photodetector (PD), the WLAN OFDM signal shown in Fig. 6(a) was generated. This OFDM signal was divided into two equal WLAN MIMO signals (X1, X2) with the same RF carrier frequency 5.4 GHz by means of a RF coupler with coupling factor of 0.50. Transferring RF WLAN MIMO signals over SMF will result in severe power degradation due to fiber chromatic dispersion. RF power degradation due to the fiber dispersion was overcome by implementation of the optical single sideband (OSSB) modulation technique [22]. As such, the OSSB+Carrier modulation technique was implemented, with the MZMs used to modulate the MIMO signals (X1, X2) on two assigned carriers a and c, respectively. The subsequent results are shown in Fig. 6(b).

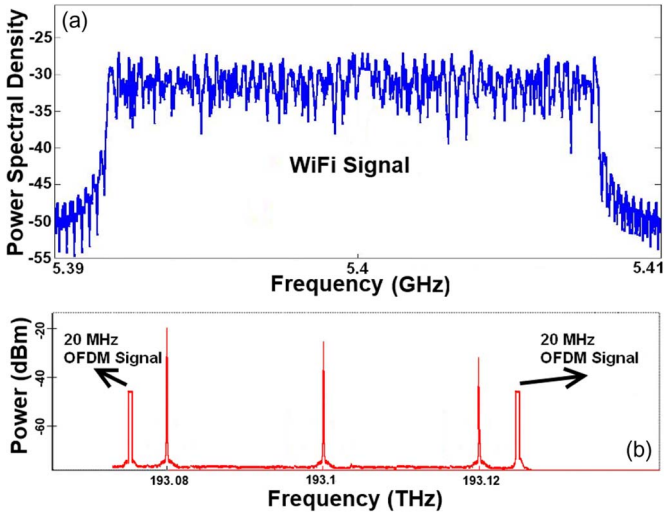

Fig. 6. (a) All optically generated OFDM signal. (b) Transmitted signal spectra to SMF.

4.2. MIMO WLAN Signals Optical Transmission

Subsequent to the previously described procedures, the modulated optical signals and the base optical carrier b were multiplexed and then amplified by an erbium-doped fiber amplifier (EDFA). This multiplexed signal with the spectral profile shown in Fig. 6(b) was next transmitted through the SMF. Specifications of the SMF included a non-linear refractive index of 2.6 $\times$ 10–20 m2/W, the fiber optic was utilized in two lengths of L $=$ 25 and 50 km, attenuation of 0.2 dB/km, dispersion of 5 ps/nm/km, differential group delay of 0.2 ps/km, effective area of 25 μm2, and a non-linear phase shift of 3 mrad. The received optical signal power was adjusted by a variable optical attenuator (VOA) and was set at $-$15 dBm. The transmitter antenna base station (TABS) comprised a demultiplexer, a polarization controller (PC) to adjust the state of the polarization, PIN photodetectors (PDs) with 0.7 A/W responsivity, electrical band pass filters (BPFs), amplifiers and multiple transmitter antennas (Tx1, Tx2) for MIMO applications. The optical downstream was demultiplexed to the two modulated optical signals and one un-modulated carrier b, after which two modulated optical signals were converted directly to electrical signals using PDs. The base carrier b was then reusable for the generation of uplink wavelength. Electrical signals were filtered on the allocated RF frequency by using BPFs.

4.3. MIMO WLAN Signals Wireless Transmission

The general V-BLAST system with Zero Forcing (ZF) detectors in fading channels as shown in Fig. 7 is considered for MIMO processing. The MIMO OFDM signals (X_{11}, X_{12}), which are identical to the transmitted signals (X1, X2) with small noise, propagated wirelessly through the MIMO channel using 2 $\times$ 2 MIMO Tx antennas designed to operate at 5.4 GHz, possessed the frequency response as shown in Fig. 7(a)–(d), and were received by wireless end users. The array type antenna was chosen in order to enhance gain values, and this MIMO array antenna covered a footprint of 45 $\times$ 45 mm^2, radiated a fixed beam in the boresight direction, and achieved a 10 dB impedance bandwidth of 20 MHz with the maximal realized gain of 23.66 dBi at 5.4 GHz. The 5.4 GHz wavelength is approximately 2.18 in. Therefore, to support diversity on a 5.4 GHz radio with two separate antennas, the antennas was spaced approximately 2.2 in. apart. Noises on the signal were mostly stemmed by the optical elements and optical link, while the PCs were used to maximize PD performance.

Propagated RF WLAN signals are received at the receiver antenna base station. The quality of digital communication signals can be assessed via calculation of error vector magnitude (EVM), in which the RF signals are amplified, analyzed and then EVM based on wireless

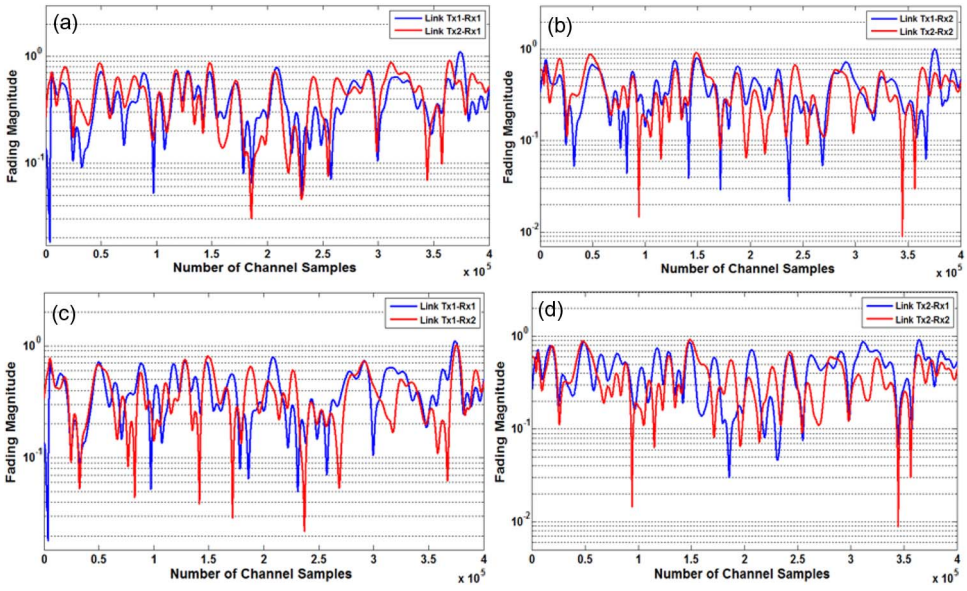

Fig. 7. MIMO channel frequency response.

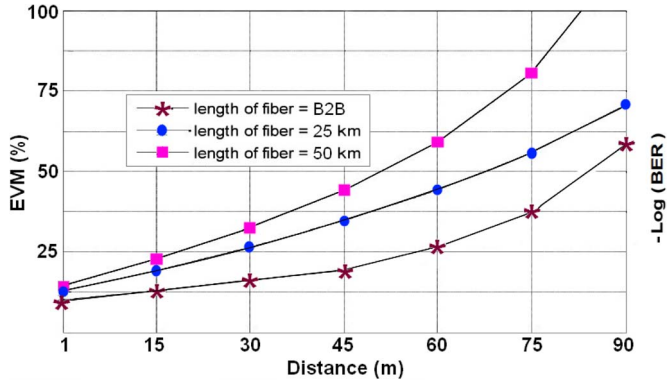

Fig. 8. EVM calculation of overall system.

channel distances is performed. The EVM results for different wireless distances and in different optical path lengths are shown in Fig. 8. According to [15], the EVM threshold for successful communication is 25% for QPSK modulation. It is clear for different optical path lengths of back to back (B2B), 25 km and 50 km there is an acceptable EVM variation for wireless distance lower than 60, 30 and 15 m respectively. Therefore it can be concluded that the transmission of both MIMO RF signals is feasible up to a 50 km SMF path length and wireless distance of 15 m. A further investigation on system performance was conducted using a bit-error-rate (BER) calculation. As illustrated in Fig. 9, the system performance was investigated under three fiber lengths (B2B, 25 km and 50 km) whereby wireless distance remained at 15 m.

In order to investigate the optical link performance, the total optical power level after amplification was adjusted with a VOA. At the threshold BER (3.8×10^{-3}) there are -21.7, -20.3, and -16.5 dBm sensitivities for Rx at fiber transmissions at B2B, 25 km and 50 km, respectively. Thereafter, power penalties of 1.4 and 5.2 dB were determined for 25 and 50 km SMF transmissions, respectively, at the BER threshold. The presented system and results demonstrate the feasibility of using the MRR system to generate both single and multi-carriers that can be applied to the optical generation of WLAN MIOMO signals.

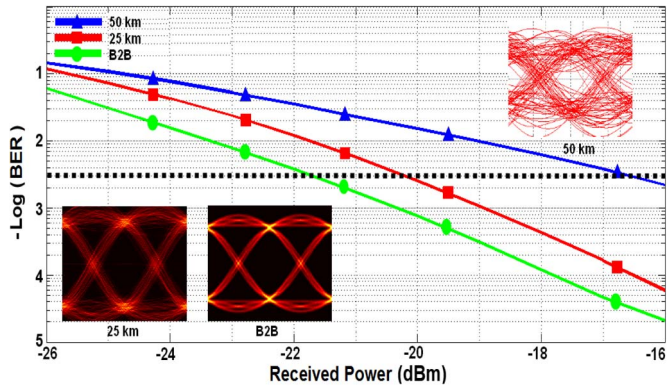

Fig. 9. System performance under B2B, 25, and 50 km fiber lengths. Eye diagrams for B2B, 25 km, and 50 km.

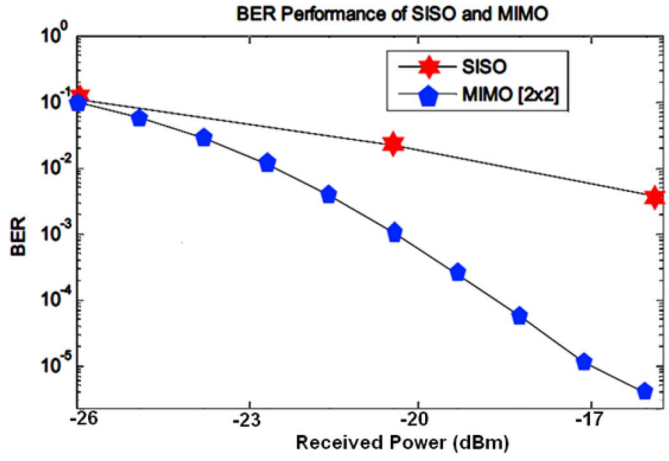

Fig. 10. BER vs SNR for SISO and MIMO.

5. MIMO vs SISO

Fig. 10 shows the BER performance of single-input and single-output (SISO) and MIMO and QPSK modulation scheme for a B2B optical link and 15 m propagation through a wireless channel.

A SISO configuration, which was single antenna for transmitter and single antenna for the receiver end, had no diversity on either end, yet the MIMO arrangement, which exploited two transmitter antennae and two receiver antennae, allowed for diversity to exist at both end of the wireless communication process. Consequently, the BER performance of MIMO system was better than SISO over the same received power.

6. Conclusion

A series of MRRs incorporated with an add/drop filter system were used to generate THz frequency band signals. Filtering of the input pulse within the system allowed for generation of single- and multi-soliton pulses to be used in a described MIMO-OFDM-RoF communication system. A soliton THz range of 193–193.2 THz at frequencies of 193.08, 193.1, and 193.12 THz with FSR of 20 GHz was achieved, which provided the carriers necessary for MIMO RF signal transportation. All-optically generated WLAN signals were investigated in RoF applications.

Results confirmed that two 5.4 GHz MIMO-WLAN signals were generated and transported through the SMF optical link and 2 × 2 MIMO channel. EVM and BER calculations for the overall channels confirmed the feasibility of MIMO transportation. The authors anticipate the work described here will spur further development in this field.

References

[1] Q. Tang and X. Xu, "Wireless multimedia communication requirements for police and PDT+ LTE+ 3G solution," in *Advances on Digital Television and Wireless Multimedia Communications*, Berlin, Germany: Springer-Verlag, 2012, pp. 341–346.

[2] D. Wake *et al.*, "A comparison of radio over fiber link types for the support of wideband radio channels," *J. Lightw. Technol.*, vol. 28, no. 16, pp. 2416–2422, Aug. 2010.

[3] M. D. Renzo, H. Haas, and P. M. Grant, "Spatial modulation for multiple-antenna wireless systems: A survey," *IEEE Commun. Mag.*, vol. 49, no. 12, pp. 182–191, Dec. 2011.

[4] Q. Li *et al.*, "MIMO techniques in WiMAX and LTE: A feature overview," *IEEE Commun. Mag.*, vol. 48, no. 5, pp. 86–92, May 2010.

[5] C. Lim *et al.*, "Fiber-wireless networks and subsystem technologies," *J. Lightw. Technol.*, vol. 28, no. 4, pp. 390–405, Feb. 2010.

[6] M. Sauer, A. Kobyakov, and J. George, "Radio over fiber for picocellular network architectures," *J. Lightw. Technol.*, vol. 25, no. 11, pp. 3301–3320, Nov. 2007.

[7] D. T. Pham, M. K. Hong, J. M. Joo, and S. K. Han, "Heterogeneous gigabit orthogonal frequency division multiplexing/radio over fiber transmissions of wired and wireless signals using a reflective semiconductor optical amplifier and single-arm mach-zehnder modulator," *Microw. Opt. Technol. Lett.*, vol. 54, no. 8, pp. 1954–1958, Aug. 2012.

[8] G. L. Stuber *et al.*, "Broadband MIMO-OFDM wireless communications," *Proc. IEEE*, vol. 92, no. 2, pp. 271–294, Feb. 2004.

[9] L. Deng *et al.*, "2 × 2 MIMO-OFDM Gigabit fiber-wireless access system based on polarization division multiplexed WDM-PON," *Opt. Exp.*, vol. 20, no. 4, pp. 4369–4375, Feb. 2012.

[10] T. Yamakami, T. Higashino, K. Tsukamoto, and S. Komaki, "An experimental investigation of applying MIMO to RoF ubiquitous antenna system," in *Proc. Int. Top. Meet. Microw. Photon. Jointly Held 2008 Asia-Pacific Microw. Photon. Conf. mwp/apmp*, 2008, pp. 201–204.

[11] C.-X. Wang *et al.*, "Cooperative MIMO channel models: A survey," *IEEE Commun. Mag.*, vol. 48, no. 2, pp. 80–87, Feb. 2010.

[12] Y. Benlachtar *et al.*, "Generation of optical OFDM signals using 21.4 GS/s real time digital signal processing," *Opt. Exp.*, vol. 17, no. 20, pp. 17 658–17 668, Sep. 2009.

[13] Q. Yang, S. Chen, Y. Ma, and W. Shieh, "Real-time reception of multi-gigabit coherent optical OFDM signals," *Opt. Exp.*, vol. 17, no. 10, pp. 7985–7992, May 2009.

[14] H. Chen, M. Chen, and S. Xie, "All-optical sampling orthogonal frequency-division multiplexing scheme for high-speed transmission system," *J. Lightw. Technol.*, vol. 27, no. 21, pp. 4848–4854, Nov. 2009.

[15] Z. Wang, K. S. Kravtsov, Y.-K. Huang, and P. R. Prucnal, "Optical FFT/IFFT circuit realization using arrayed waveguide gratings and the applications in all-optical OFDM system," *Opt. Exp.*, vol. 19, no. 5, pp. 4501–4512, Feb. 2011.

[16] M. Spyropoulou, N. Pleros, and A. Miliou, "SOA-MZI-based nonlinear optical signal processing: A frequency domain transfer function for wavelength conversion, clock recovery, and packet envelope detection," *IEEE J. Quantum Electron.*, vol. 47, no. 1, pp. 40–49, Jan. 2011.

[17] S. Lin and K. B. Crozier, "Planar silicon microrings as wavelength-multiplexed optical traps for storing and sensing particles," *Lab Chip*, vol. 11, pp. 4047–4051, 2011.

[18] J. P. Gordon and L. F. Mollenauer, "Effects of fiber nonlinearities and amplifier spacing on ultra-long distance transmission," *J. Lightw. Technol.*, vol. 9, no. 2, pp. 170–173, Feb. 1991.

[19] M. A. Jalil *et al.*, "Embedded nanomicro syringe on chip for molecular therapy," *Int. J. Nanomedicine*, vol. 6, p. 2925, 2011.

[20] N. Suwanpayak, M. A. Jalil, M. Aziz, J. Ali, and P. Yupapin, "Molecular buffer using a PANDA ring resonator for drug delivery use," *Int. J. Nanomedicine*, vol. 6, pp. 575–580, 2011.

[21] S. Mitatha *et al.*, "Proposal for Alzheimer's diagnosis using molecular buffer and bus network," *Int. J. Nanomedicine*, vol. 6, pp. 1209–1216, 2011.

[22] C. Hong *et al.*, "Single-sideband modulation based on an injection-locked DFB laser in radio-over-fiber systems," *IEEE Photon. Technol. Lett.*, vol. 22, no. 7, pp. 462–464, Apr. 2010.

[23] I. S. Amiri, S. E. Alavi, and J. Ali, "High capacity soliton transmission for indoor and outdoor communications using integrated ring resonators," *Int. J. Commun. Syst.*, 2013, DOI: 10.1002/dac.2645.

[24] I. S. Amiri, S. Soltanmohammadi, A. Shahidinejad, and J. Ali, "Optical quantum transmitter with finesse of 30 at 800-nm central wavelength using microring resonators," *Opt. Quantum Electron.*, vol. 45, no. 10, pp. 1095–1105, Oct. 2013.

[25] S. E. Alavi *et al.*, "All optical OFDM generation for IEEE802.11a based on soliton carriers using MicroRing resonators" *IEEE Photon. J.*, vol. 6, no. 1, Feb. 2014, Art. ID. 7900109.

[26] I. S. Amiri *et al.*, "IEEE 802.15.3c WPAN standard using millimeter optical soliton pulse generated by a panda ring resonator," *IEEE Photon. J.*, vol. 5, no. 5, Oct. 2013, Art. ID. 7901912.